



MINISTÈRE
DE L'ÉDUCATION
NATIONALE

EAD SVT 2

SESSION 2019

**AGRÉGATION
CONCOURS EXTERNE SPÉCIAL**

**Section : SCIENCES DE LA VIE,
SCIENCES DE LA TERRE ET DE L'UNIVERS**

ÉTUDE DE DOSSIER SCIENTIFIQUE

Durée : 4 heures

L'usage de tout ouvrage de référence, de tout autre dictionnaire et de tout matériel électronique (y compris la calculatrice) est rigoureusement interdit.

Si vous repérez ce qui vous semble être une erreur d'énoncé, vous devez le signaler très lisiblement sur votre copie, en proposer la correction et poursuivre l'épreuve en conséquence. De même, si cela vous conduit à formuler une ou plusieurs hypothèses, vous devez la (ou les) mentionner explicitement.

NB : Conformément au principe d'anonymat, votre copie ne doit comporter aucun signe distinctif, tel que nom, signature, origine, etc. Si le travail qui vous est demandé consiste notamment en la rédaction d'un projet ou d'une note, vous devrez impérativement vous abstenir de la signer ou de l'identifier.

Tournez la page S.V.P.

A

INFORMATION AUX CANDIDATS

Vous trouverez ci-après les codes nécessaires vous permettant de compléter les rubriques figurant en en-tête de votre copie.

Ces codes doivent être reportés sur chacune des copies que vous remettrez.

Concours	Section/option	Epreuve	Matière
EAD	1600D	102	8085

La teneur en CO₂ de l'atmosphère : marqueur des flux entre la biosphère et les autres réservoirs du cycle de carbone.

En vous basant sur le dossier scientifique proposé et vos connaissances, vous traiterez du sujet tel que libellé ci-dessus, dans une dissertation construite et raisonnée.

L'exposé comprendra obligatoirement :

- une version retravaillée en français et adaptée à un public de l'enseignement secondaire d'une des figures du dossier,
- un glossaire de 10 mots-clés, dont vous donnerez les définitions.

Le choix de la figure didactisée, des mots-clés du glossaire et la rigueur de leurs définitions seront évalués. Le choix d'une utilisation partielle des documents du dossier sera à justifier.

Le dossier scientifique comporte 13 documents tirés de références scientifiques, les termes ambigus, acronymes et termes d'anglais non usuels ont été définis et traduits. Les légendes des figures ont été conservées telles quelles, les éventuels renvois à d'autres figures ou tableaux ne sont pas valides.

Si vous désirez joindre un document du dossier annoté à votre copie, vous êtes tenu de le coller dans votre copie, seuls les feuillets anonymisés étant autorisés.

La teneur en CO₂ de l'atmosphère : marqueur des flux entre la biosphère et les autres réservoirs du cycle de carbone.

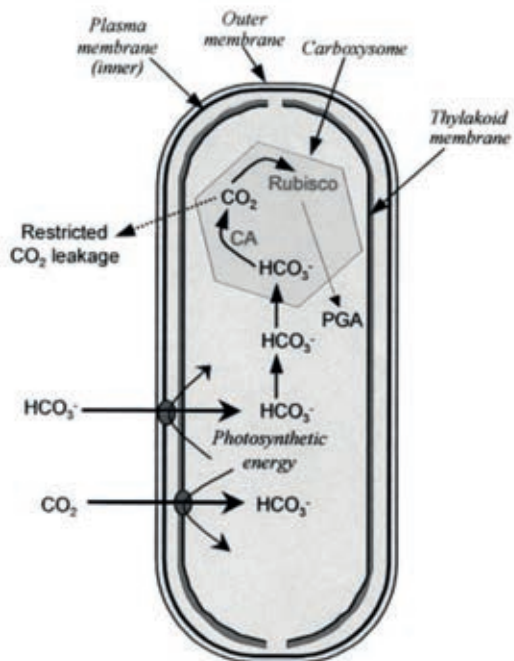
DOCUMENT 1 : Les mécanismes de concentration du carbone chez les cyanobactéries.

CCM : Carbon Concentration Mechanism

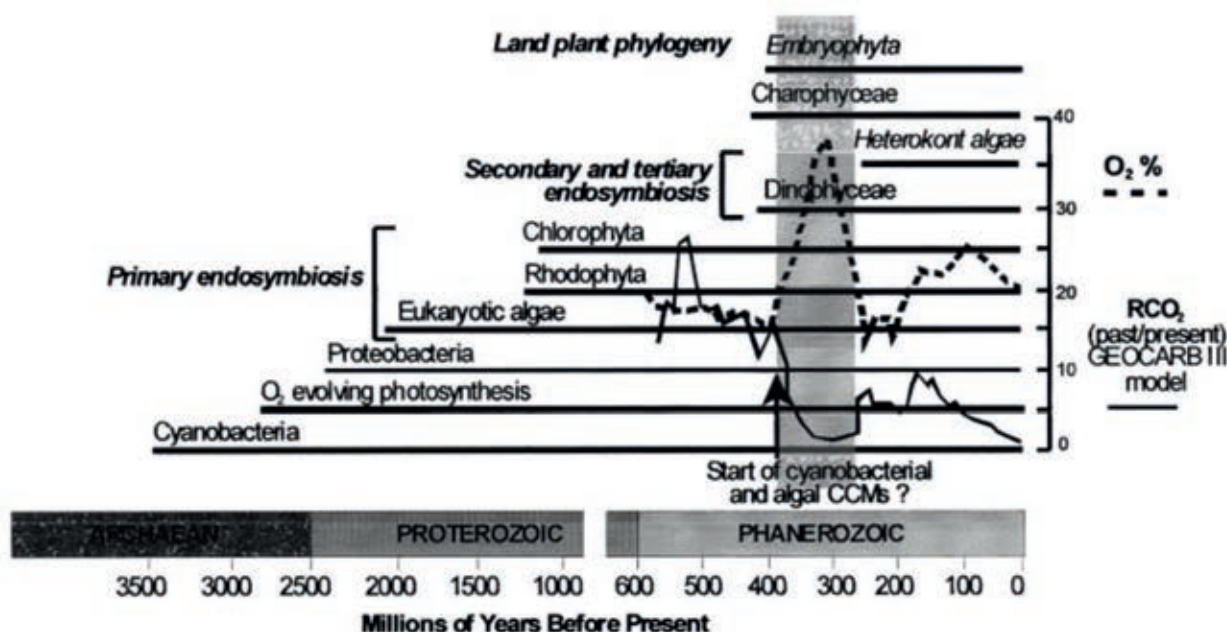
Leakage : fuite

GEOCARB III : Courbe synthétique (modélisation) de l'évolution de la pCO₂ (Berner et Kothavala, 2001)

Source : Badger M. R. et G.D. Price, 2003, CO₂ concentrating mechanisms in cyanobacteria: molecular components, their diversity and evolution *Journal of Experimental Botany*, Vol. 54, No. 383, pp. 609-622,



1A A generalized model for the cyanobacterial CCM. Shown on the figure are the Rubisco-containing carboxysomes with the carboxysomal carbonic anhydrase (CA) and an associated diffusional resistance to CO₂ efflux. The accumulation of HCO₃⁻ in the cytosol is achieved through the action of a number of CO₂ and HCO₃⁻ uptake systems.



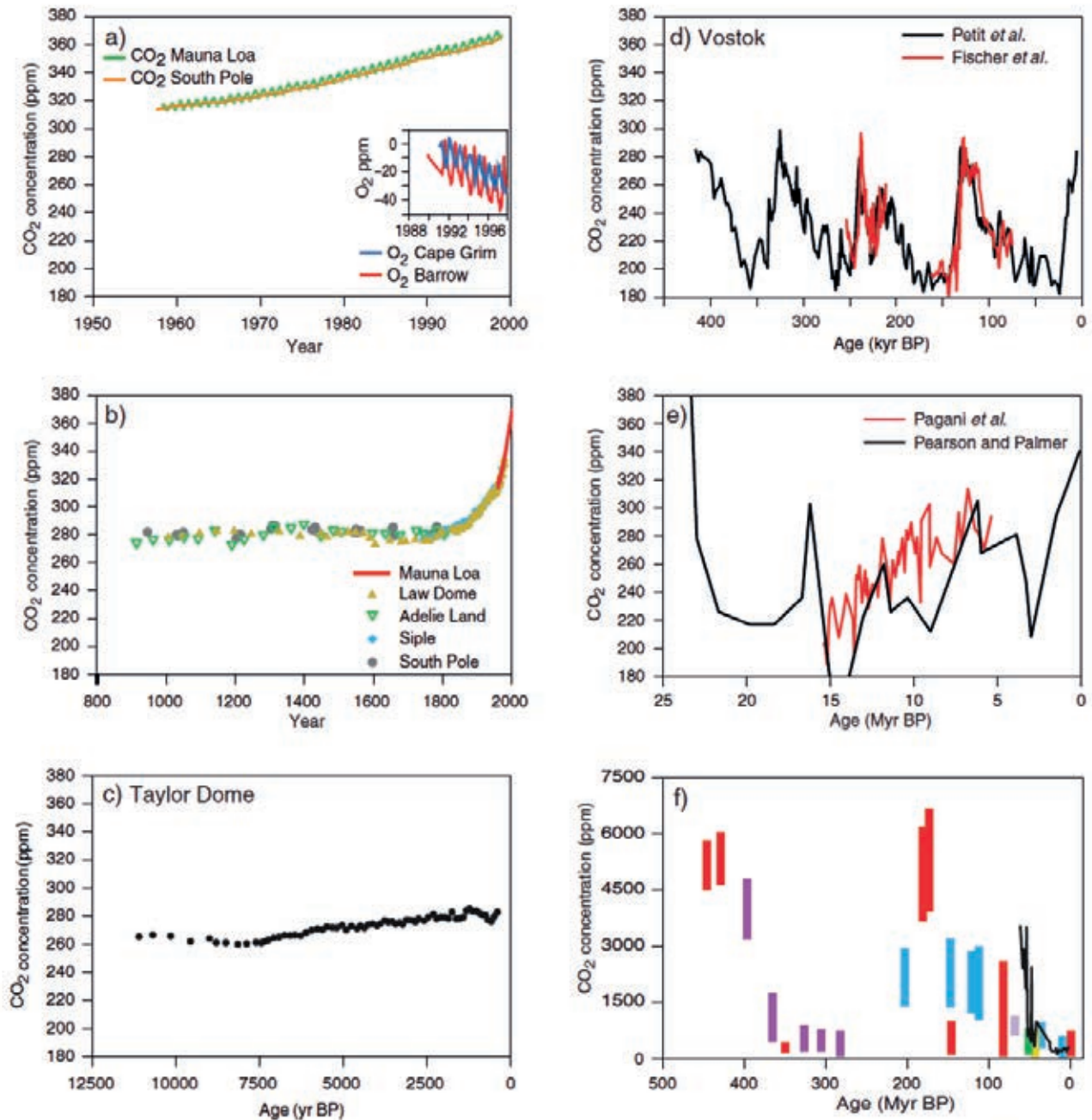
1B The evolution of photosynthetic cyanobacteria, algae, higher plants, and chemoautotrophic proteobacteria over the past 3.5 billion years. (drawn with reference to Raven, 1997b, and Badger *et al.*, 2002). Also shown on the graph are the proposed changes in CO₂ and O₂ during the Phanerozoic period (Berner, 2001; Berner and Kothavala, 2001). CO₂ is shown as the ratio of past to present levels (R_{CO_2}) while O₂ is shown as percentage content. The shaded section indicates the period of CO₂ limitation combined with O₂ increase that may have initiated the development of CCMs in aquatic photosynthetic organisms.

La teneur en CO₂ de l'atmosphère : marqueur des flux entre la biosphère et les autres réservoirs du cycle de carbone.

DOCUMENT 2 : Les estimations de la pCO₂ atmosphérique à différentes échelles de temps

Le code couleur de la figure f correspond aux différents types de données utilisées.

Source : IPCC, 2001: *Climate Change 2001: The Scientific Basis. Contribution of Working Group I to the Third Assessment Report of the Intergovernmental Panel on Climate Change* [Houghton, J.T., Y. Ding, D.J. Griggs, M. Noguer, P.J. van der Linden, X. Dai, K. Maskell, and C.A. Johnson (eds.)]. Cambridge University Press, Cambridge, United Kingdom and New York, NY, USA, 881pp.

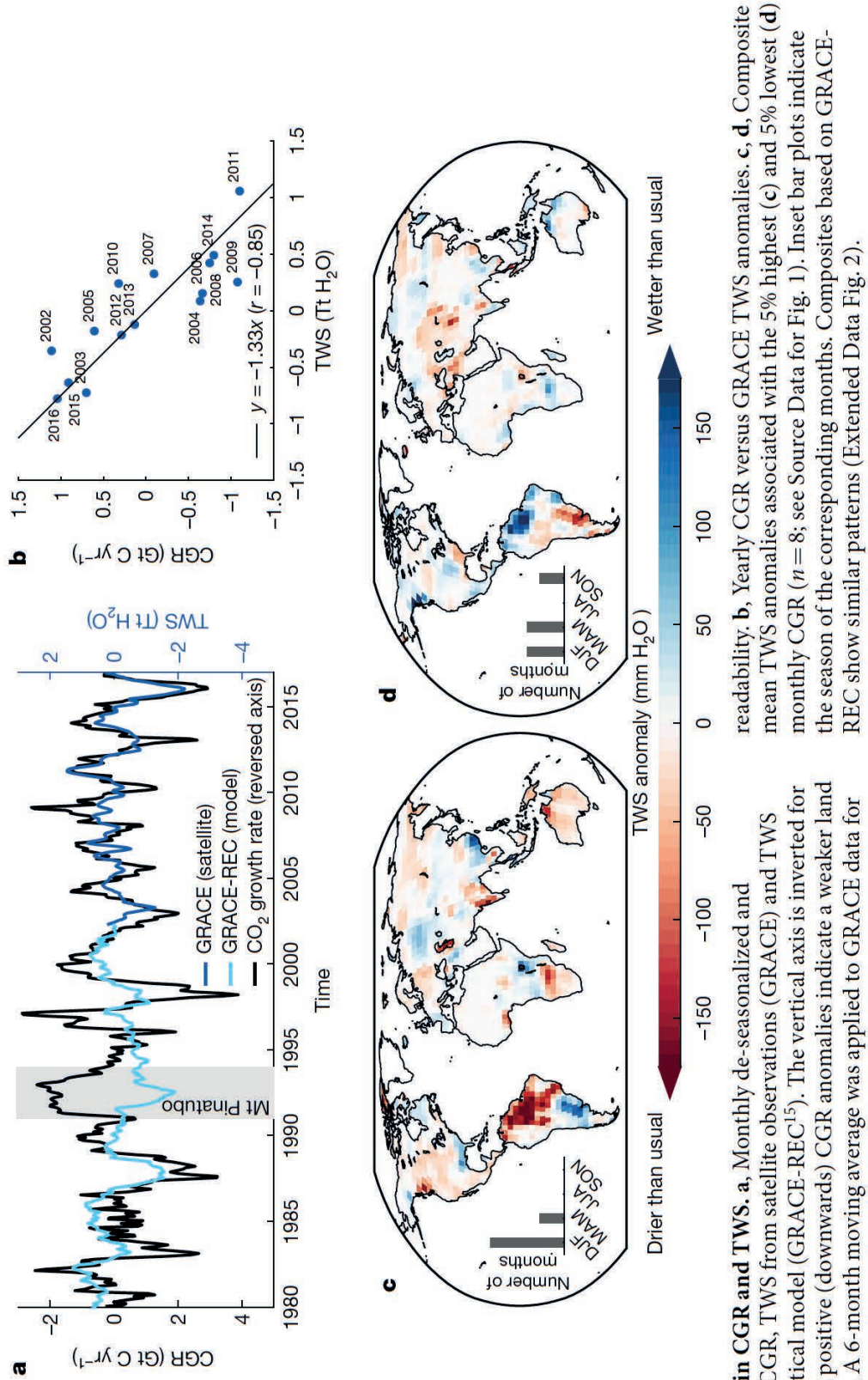


Variations in atmospheric CO₂ concentration on different time-scales. (a) Direct measurements of atmospheric CO₂ concentration (Keeling and Whorf, 2000), and O₂ from 1990 onwards (Battle *et al.*, 2000). O₂ concentration is expressed as the change from an arbitrary standard. (b) CO₂ concentration in Antarctic ice cores for the past millenium (Siegenthaler *et al.*, 1988; Neftel *et al.*, 1994; Barnola *et al.*, 1995; Etheridge *et al.*, 1996). Recent atmospheric measurements at Mauna Loa (Keeling and Whorf, 2000) are shown for comparison. (c) CO₂ concentration in the Taylor Dome Antarctic ice core (Indermühle *et al.*, 1999). (d) CO₂ concentration in the Vostok Antarctic ice core (Petit *et al.*, 1999; Fischer *et al.*, 1999). (e) Geochemically inferred CO₂ concentrations, from Pagani *et al.* (1999a) and Pearson and Palmer (2000). (f) Geochemically inferred CO₂ concentrations: coloured bars represent different published studies cited by Berner (1997). The data from Pearson and Palmer (2000) are shown by a black line. (BP = before present.)

DOCUMENT 3 : pCO₂ atmosphérique et propriétés des sols

IAV : Inter-Annual Variability, CGR : Carbon Growth Rate / taux d'augmentation du carbone, TWS : Terrestrial Water Storage / Réserve en eau des sols, GRACE : Gravity Recovery and Climate Experiment / Campagne de gravimétrie satellitaire (2002 - 2017), GRACE-REC : modèle gravimétrique tiré des données de GRACE, sink : puits.

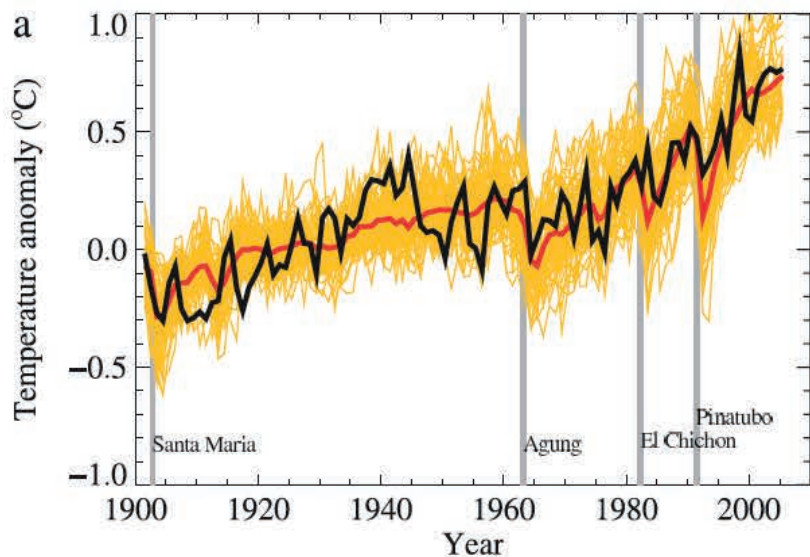
Source : Humphrey V. , J. Zscheischler, P. Ciais, L. Gudmundsson, S. Sitch & S. I. Seneviratne, 2018, Sensitivity of atmospheric CO₂ growth rate to observed changes in terrestrial water storage, Nature, vol 560 n° 628, doi.org/10.1038/s41586-018-0424-4



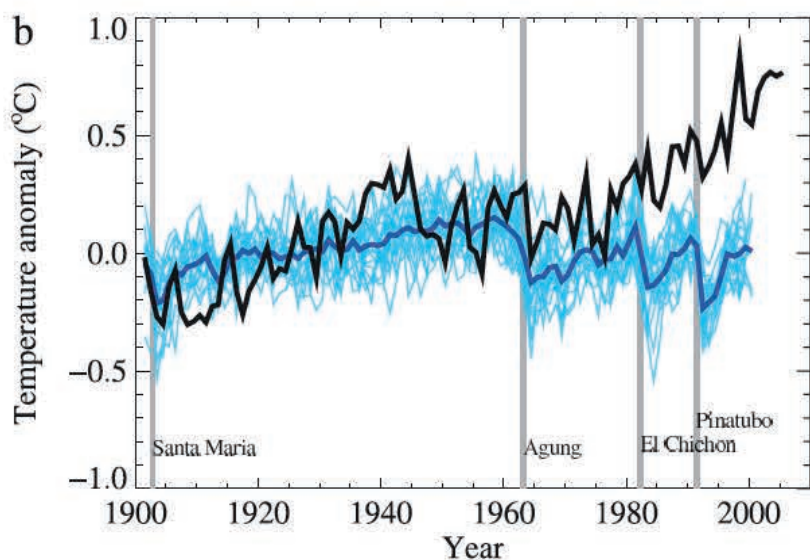
IAV in CGR and TWS. **a**, Monthly de-seasonalized and de-trended CGR, TWS from satellite observations (GRACE) and TWS from a statistical model (GRACE-REC¹⁵). The vertical axis is inverted for CGR so that positive (downwards) CGR anomalies indicate a weaker land carbon sink. A 6-month moving average was applied to GRACE data for readability. **b**, Yearly CGR versus GRACE TWS anomalies. **c, d**, Composite mean TWS anomalies associated with the 5% highest (c) and 5% lowest (d) monthly CGR ($n = 8$; see Source Data for Fig. 1). Inset bar plots indicate the season of the corresponding months. Composites based on GRACE-REC show similar patterns (Extended Data Fig. 2).

DOCUMENT 4 : Données et modèles d'anomalies de températures moyennes de surface pour le XXe siècle.

AOGCM : Atmosphere-Ocean General Circulation Model



Source : Hegerl, G.C., F. W. Zwiers, P. Braconnot, N.P. Gillett, Y. Luo, J.A. Marengo Orsini, N. Nicholls, J.E. Penner and P.A. Stott, 2007: Understanding and Attributing Climate Change. In: Climate Change 2007: The Physical Science Basis. Contribution of Working Group I to the Fourth Assessment Report of the Intergovernmental Panel on Climate Change [Solomon, S., D. Qin, M. Manning, Z. Chen, M. Marquis, K.B. Averyt, M. Tignor and H.L. Miller (eds.)]. Cambridge University Press, Cambridge, United Kingdom and New York, NY, USA.



Comparison between global mean surface temperature anomalies (°C) from observations (black) and AOGCM simulations forced with (a) both anthropogenic and natural forcings and (b) natural forcings only. All data are shown as global mean temperature anomalies relative to the period 1901 to 1950, as observed (black, Hadley Centre/Climatic Research Unit gridded surface temperature data set (HadCRUT3); Brohan et al., 2006) and, in (a) as obtained from 58 simulations produced by 14 models with both anthropogenic and natural forcings. The multi-model ensemble mean is shown as a thick red curve and individual simulations are shown as thin yellow curves. Vertical grey lines indicate the timing of major volcanic events. Those simulations that ended before 2005 were extended to 2005 by using the first few years of the IPCC Special Report on Emission Scenarios (SRES) A1B scenario simulations that continued from the respective 20th-century simulations, where available. The simulated global mean temperature anomalies in (b) are from 19 simulations produced by five models with natural forcings only. The multi-model ensemble mean is shown as a thick blue curve and individual simulations are shown as thin blue curves. Simulations are selected that do not exhibit excessive drift in their control simulations (no more than 0.2°C per century). Each simulation was sampled so that coverage corresponds to that of the observations. Further details of the models included and the methodology for producing this figure are given in the Supplementary Material, Appendix 9.C. After Stott et al. (2006b).

DOCUMENT 5 : Arbre phylogénétique simplifié des Embryophytes

Source : Kenrick, P. et P. R. Crane, 1997, *The origin and early evolution of plants on land, Nature, Vol. 389, n° 4.*

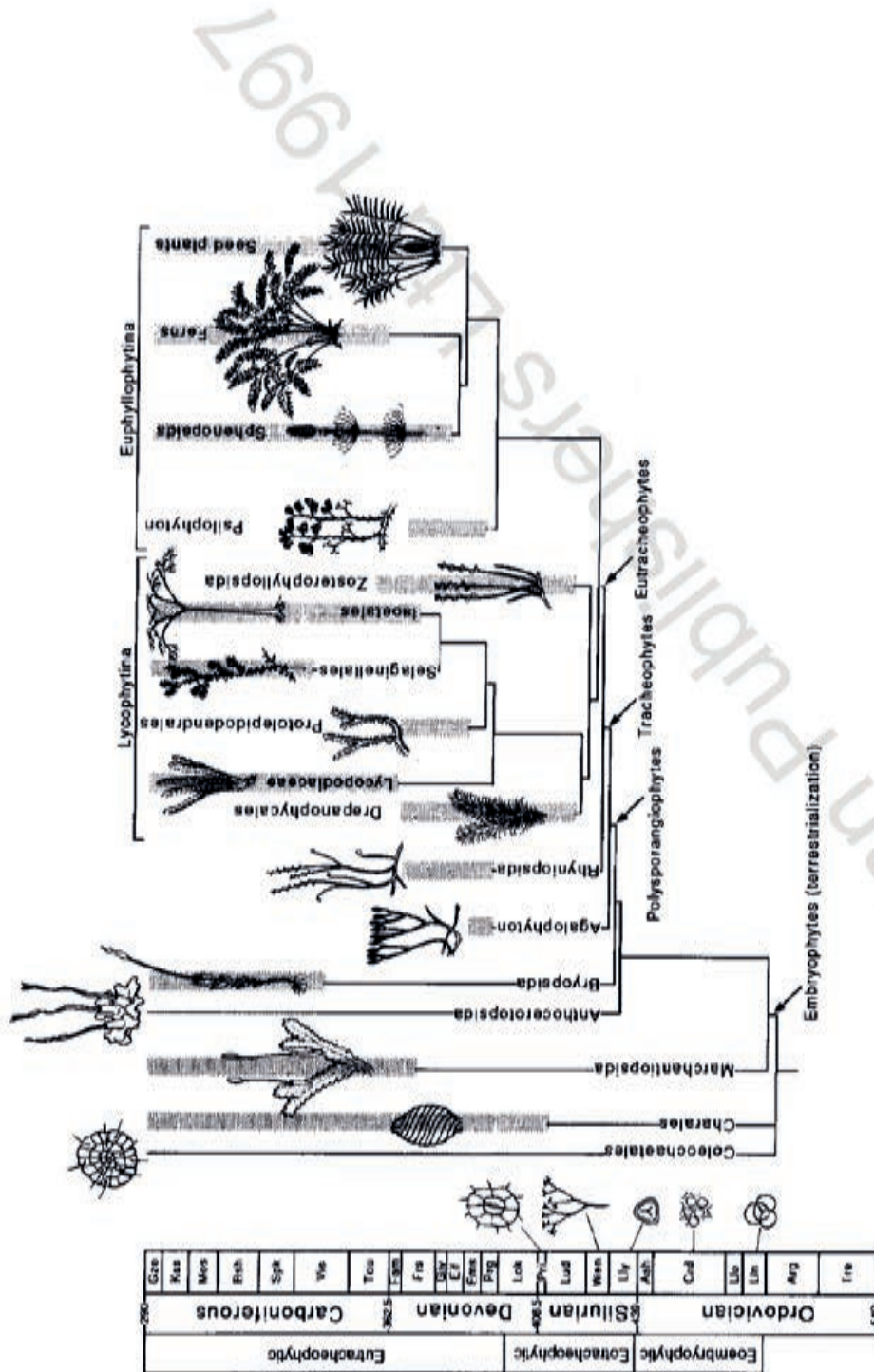


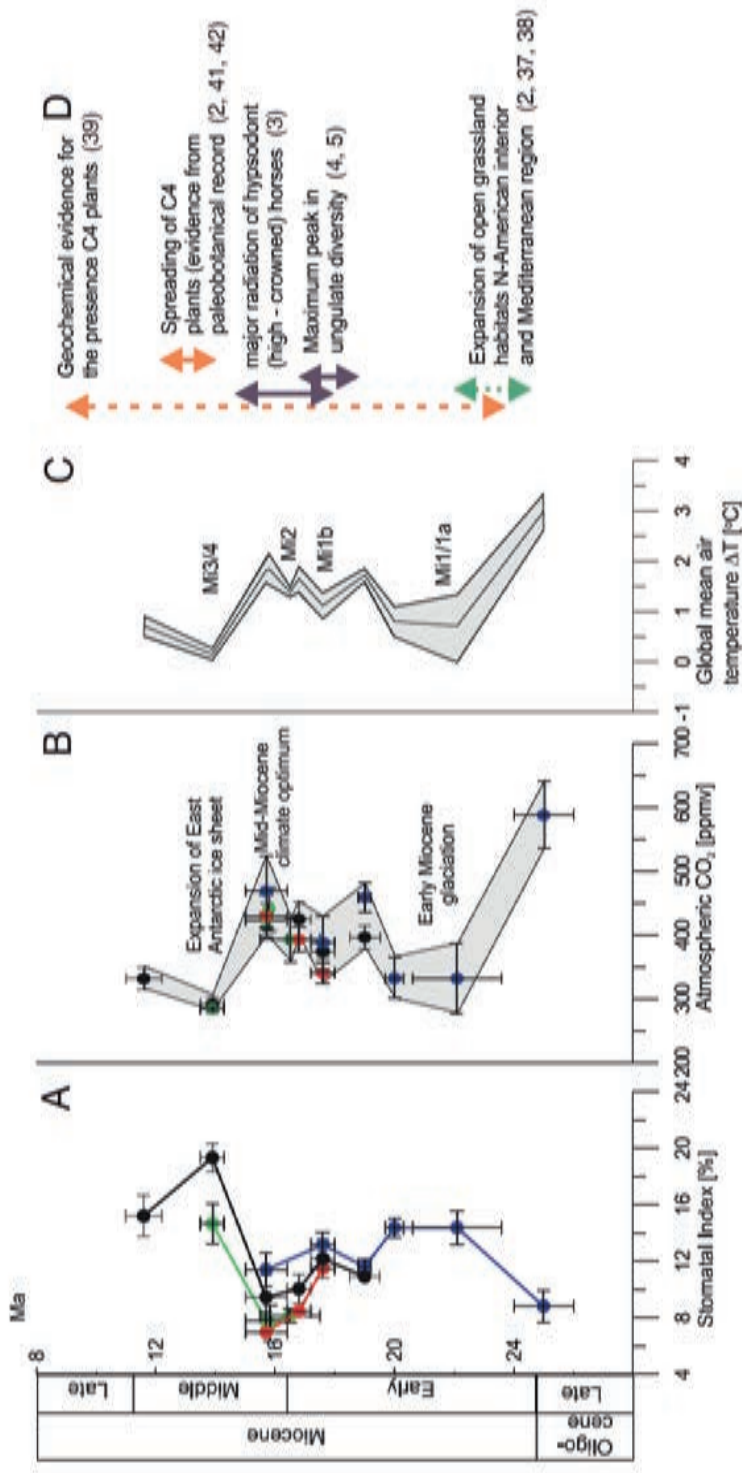
Figure 4 Simplified phylogenetic tree showing the minimum stratigraphic ranges of selected groups based on megafossils (thick bars) and their minimum implied range extensions (thin lines). Also illustrated alongside time scale are minimum age estimates for the appearance of certain important land-plant features (from the bottom: spore tetrads, cuticles, single trilete spores, megafossils and stomates). The first unequivocal record of charophycean algae is based on calcified charalean oogonia (female sexual organs) from the Late Silurian (Pridoli, ~410 Myr)⁶² and distinctive gametophytes from the Early Devonian Rhynie Chert⁶⁴. Proposed similarities between living Coleochaete and Early Devonian Parkia remain to be confirmed⁶⁴. Note that megafossil evidence for vascular plants precedes megafossil evidence of bryophytes and charophycean algae. Confirmation that the Early Devonian Sporogonites is a plant at the bryophyte grade could help to reduce this discrepancy. Tre, Tremadoc; Arg, Arenig; Lln, Llanvirn; Llo, Llandoilgo; Crd, Caradoc; Ash, Ashgill; Lly, Llandowery; Wen, Wenlock; Lud, Ludlow; Pri, Pridoli; Lok, Lochkovian (Gedinnian); Prg, Pragian (Siegenian); Ems, Emsian; Eif, Eifelian; Giv, Givetian; Frs, Frasnian; Fam, Famennian; Tou, Tournaisian; Vis, Viséan; Spk, Serpukhovian; Bsh, Bashkirian; Mos, Moscovian; Kas, Kasimovian; Gze, Gzelian.

La teneur en CO₂ de l'atmosphère : marqueur des flux entre la biosphère et les autres réservoirs du cycle de carbone.

DOCUMENT 6 : pCO₂ atmosphérique et grands événements des écosystèmes terrestres au Miocène.

SI : Stomatal Index. Les numéros entre parenthèses renvoient aux sources des données.

Source : Kurschner W. M., Z. Koacek, and D. L. Dilcher, 2008, *The impact of Miocene atmospheric carbon dioxide fluctuations on climate and the evolution of terrestrial ecosystems*, PNAS, Vol. 105 n°2, P 449-453

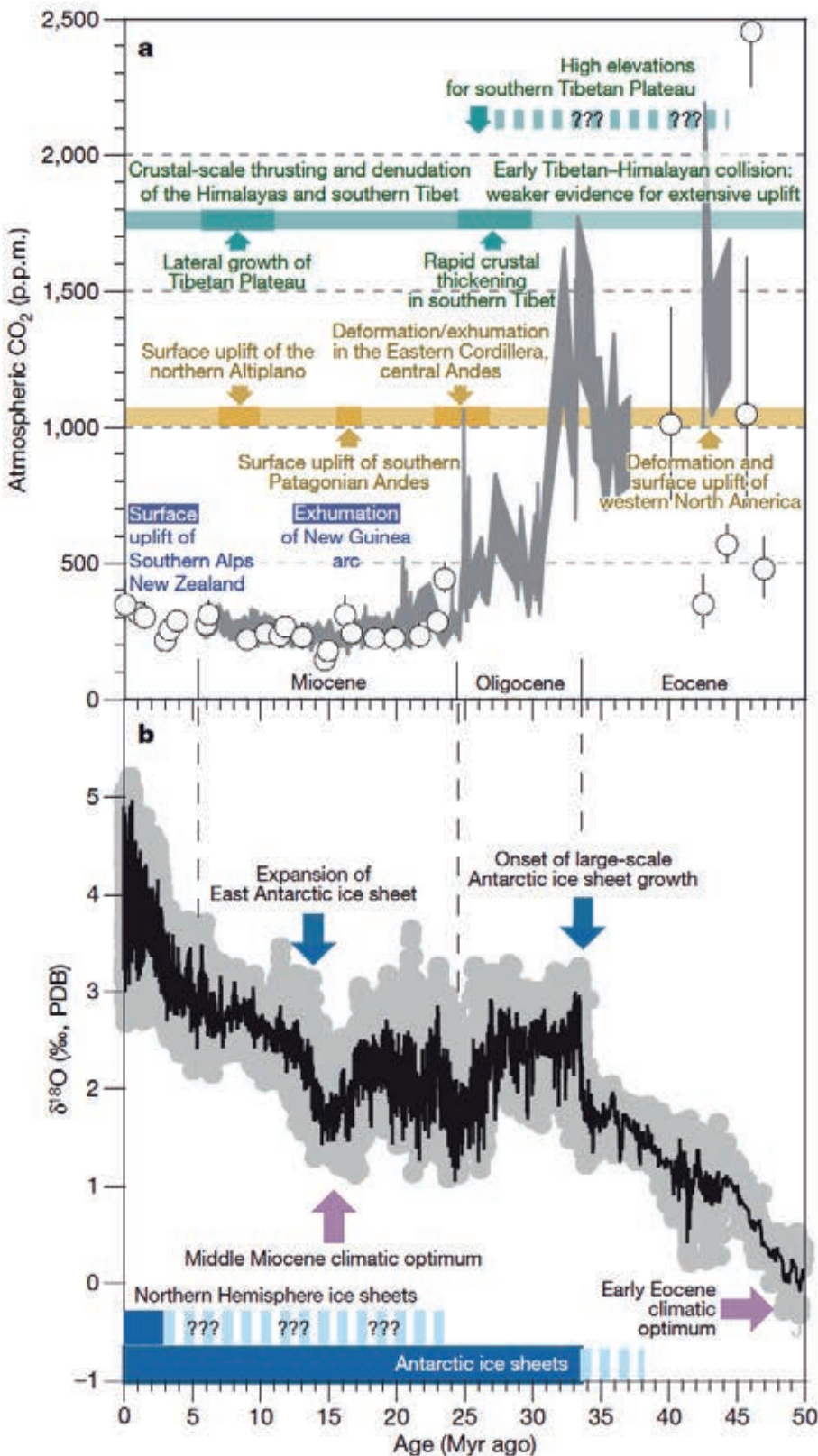


Late Oligocene–Miocene stomatal records, inferred atmospheric CO₂ fluctuations, and effects on global temperature compared with major events in terrestrial ecosystems. (A) SI of fossil leaf remains between 25 and 12 Ma (late Oligocene until late middle Miocene. For a list of locations and their age assessment, see SI Table 3). The lines represent trends in *St. blue*, *L. pseudoprinceps*; black, *L. nobilis*; red, *O. foeters*; green, *G. biloba*. The values represent means per stratigraphic unit, with error bars indicating the standard deviation of the SI. The age error bars indicate the minimum and maximum ages of the sample. The stratigraphic framework is established by vertebrate biostratigraphy and magnetostratigraphy (see also SI Table 3). (B) Reconstructed late Oligocene–middle Miocene CO₂ levels based on individually calibrated tree species. The error bars indicate the envelope as determined by the minimum and maximum CO₂ levels inferred from all individual samples per stratigraphic unit. (C) Modeled temperature departure of global mean surface temperature from present day, calculated from mean CO₂ estimates by using a CO₂–temperature sensitivity study (46). Also indicated are the major Miocene climate key events and the position of the Miocene cooling events MI1/1a, MI1b, MI2, and MI3/4 known from the marine oxygen isotope record (1). The effects of pCO₂ level changes on the global mean land surface temperature were estimated assuming a radiative relationship between CO₂ mixing and global air temperature inferred from climate–CO₂ sensitivity models expressed as $\Delta T = 4 \ln(C/CO_0)$, where C is the mixing ratio and CO₀ is the preindustrial CO₂ mixing ratio of 278 ppmv (46). (D) Major events in the terrestrial ecosystems in response to the Miocene CO₂ trends, such as changes in terrestrial herbivore communities (3–5), the expansion of Miocene grasslands (2, 37, 38), and evidence for C₄ biomass from paleosols (43).

La teneur en CO₂ de l'atmosphère : marqueur des flux entre la biosphère et les autres réservoirs du cycle de carbone.

DOCUMENT 7 : pCO₂ atmosphérique, grands évènements tectoniques et évolution climatique au Cénozoïque.

Uplift : surrection, ice sheet : inlandsis.



Source : Pagani M., K. Caldeira, R. Berner & D. J. Beerling, 2009, *The role of terrestrial plants in limiting atmospheric CO₂ decline over the past 24 million years*, *Nature*, Vol. 460, doi:10.1038/nature08133

Figure 1 | The Earth's CO₂, tectonic and climatic history over the past 50 Myr. **a**, Proxy records of long-term changes in atmospheric CO₂ concentration. Shaded bands represent a range of alkenone-based atmospheric CO₂ estimates⁸. Open circles represent CO₂ estimates from boron isotope-pH reconstructions¹³. **b**, Long-term δ¹⁸O record from benthic foraminifera¹². p.p.m., parts per million. PDB, Pee Dee belemnite standard.

La teneur en CO₂ de l'atmosphère : marqueur des flux entre la biosphère et les autres réservoirs du cycle de carbone.

DOCUMENT 8 : Flux de carbone entre réservoirs pour les périodes préindustrielle (Table 1) et industrielle (Table 2). Les valeurs ont été ajustées de façon à ce que les bilans de masse soient respectés.

Source : Raven, P. A., et P. G. Falkowski, 1999, *Oceanic sinks for atmospheric CO₂, Plant, Cell and Environment*, Vol.22, pp 741–755

Flux	Pg C year ⁻¹
Volcanic/tectonic to atmosphere	0.2
From atmosphere in terrestrial gross primary productivity	100.7
From land biota to atmosphere by respiration and fire	50
From soil to atmosphere by respiration	50
From soil in rivers	0.7
From atmosphere to warm surface ocean	70
From warm surface ocean to atmosphere	71.5
From warm surface ocean to biota in gross primary productivity	20
From biota to warm surface ocean in respiration	18
From atmosphere to cold surface ocean	20
From cold surface ocean to atmosphere	19
From cold surface ocean to biota in gross primary productivity	10
From biota to cold surface ocean in respiration	9
From warm surface ocean to cold surface ocean as inorganic C	19.2
From cold surface ocean to intermediate and deep waters as inorganic C	50.2
From warm surface ocean biota to intermediate and deep waters as organic C and CaCO ₃	2
From intermediate and deep waters to warm surface ocean as inorganic C	22
From cold surface ocean biota to intermediate and deep waters as organic C and CaCO ₃	1
From intermediate and deep waters to cold surface ocean as inorganic C	31
From biota in intermediate and deep waters to sediments as organic C and CaCO ₃	0.2

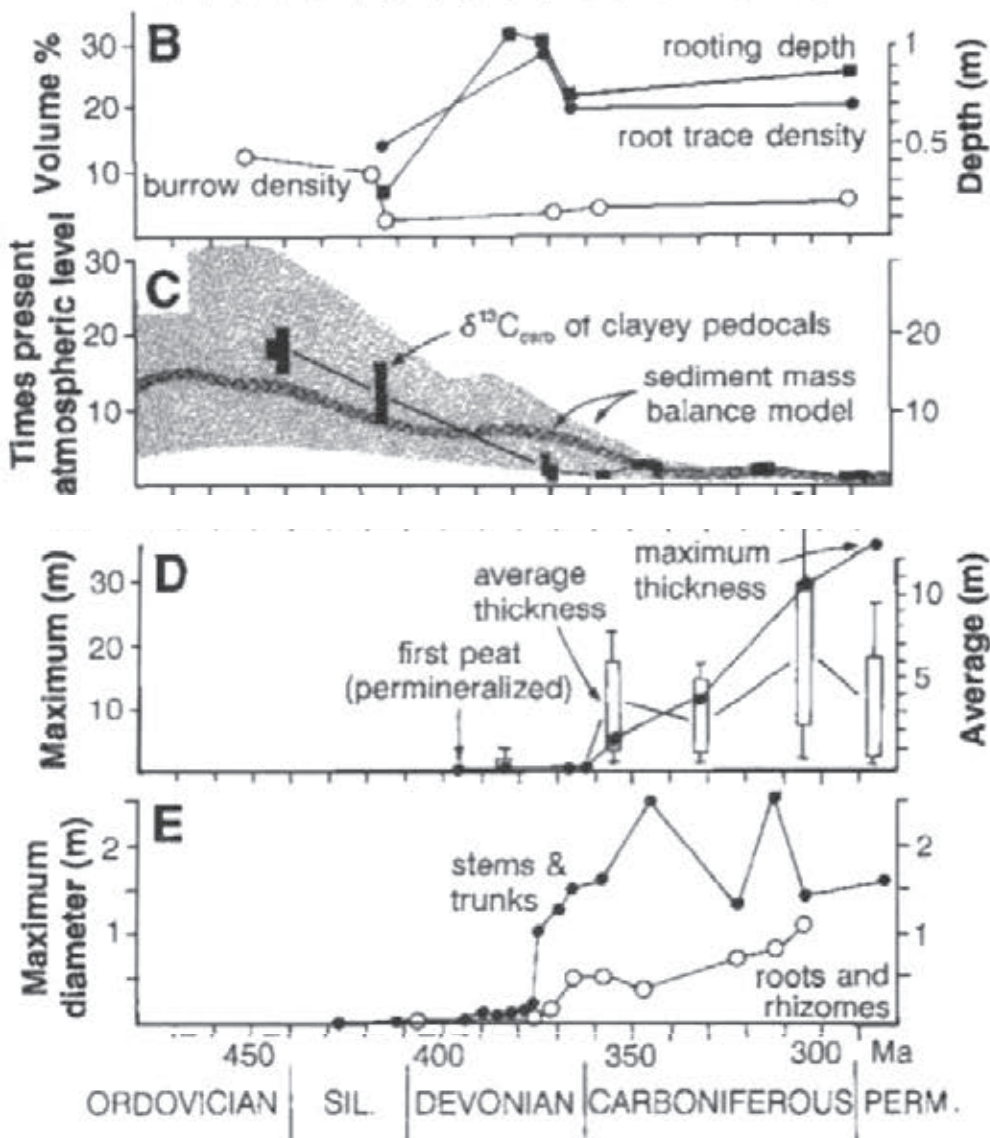
Table 1. Carbon fluxes in the pre-industrial (up to approximately 1750 AD) part of the present interglacial. Adapted from Fig. 1 of Watson & Liss (1998).

Flux	Pg C year ⁻¹
Volcanic/tectonic to atmosphere	0.2
From fossil fuels to atmosphere as CO ₂	5.4
From deforestation to atmosphere as CO ₂	2.9
From atmosphere in terrestrial gross primary productivity	102
From land biota to atmosphere by respiration and fire	50
From soil to atmosphere by respiration	50
From soil in rivers	0.7
From atmosphere to warm surface ocean	71
From warm surface ocean to atmosphere	71.5
From warm surface ocean to biota in gross primary productivity	21
From biota to warm surface ocean in respiration	18
From atmosphere to cold surface ocean	20
From cold surface ocean to atmosphere	19
From cold surface ocean to biota in gross primary productivity	10
From biota to cold surface ocean in respiration	9
From warm surface ocean to cold surface ocean as inorganic C	19.2
From cold surface ocean to intermediate and deep water as inorganic C	50.2
From warm surface ocean biota to intermediate and deep waters as organic C and CaCO ₃	2
From intermediate and deep waters to warm surface ocean as inorganic C	22
From cold surface ocean biota to intermediate and deep waters as organic C and CaCO ₃	1
From intermediate and deep waters to cold surface ocean as inorganic C	31
From biota in intermediate and deep waters to sediments as organic C and CaCO ₃	0.2

Table 2. Carbon fluxes in the present, industrial, part of the present interglacial. Adapted from Fig. 1 of Watson & Liss (1998) (our Table 1) and Siegenthaler & Sarmiento (1993).

La teneur en CO₂ de l'atmosphère : marqueur des flux entre la biosphère et les autres réservoirs du cycle de carbone.

DOCUMENT 9 : pCO₂ atmosphérique et changements long terme des paléosols et paléo-environnements de surface.



burrow : terrier,
 clayey : argileux
 peat : tourbe
 stem : tige
 coal seam : veine de charbon

Source : Gregory J. Retallack, 1997, *Forest Soils and Their Role in Devonian Global Change, Science, New Series, Vol. 276, No. 5312, pp. 583-585*

. Secular changes in paleosol features and coeval changes in the surface environments during mid-Paleozoic time (12). (B) Indices of bioturbation, including proportion of a line transect of hand specimens occupied by burrows and by roots (volume percent) (4, 28, 30, 33) and rooting depth (meters) (4, 28, 30, 33) in red clayey calcareous paleosols only. (C) Atmospheric partial pressure of CO₂ (times present atmospheric level) estimated from $\delta^{13}C$ of pedogenic carbonate (boxes) (34, 35) from red clayey calcareous paleosols, and from a sediment mass balance model [shaded area (3)]. (D) Coal thickness, including thickest coal seam and thickest average seam in successions of coals (36). (E) Maximum diameter of fossil stems and trunks and of roots and rhizomes (37, 38).

La teneur en CO₂ de l'atmosphère : marqueur des flux entre la biosphère et les autres réservoirs du cycle de carbone.

DOCUMENT 10 : pCO₂ atmosphérique et climat global

GEOCARB III : Courbe synthétique (modélisation) de l'évolution de la pCO₂ (Bernier et Kothavala, 2001)

Proxies : marqueurs

Source : Royer DL, Bernier RA, Montan ez IP, Tabor NJ, and Beerling DJ (2004) CO₂ as a primary driver of Phanerozoic climate. *GSA Today* 14(3): 4–10.

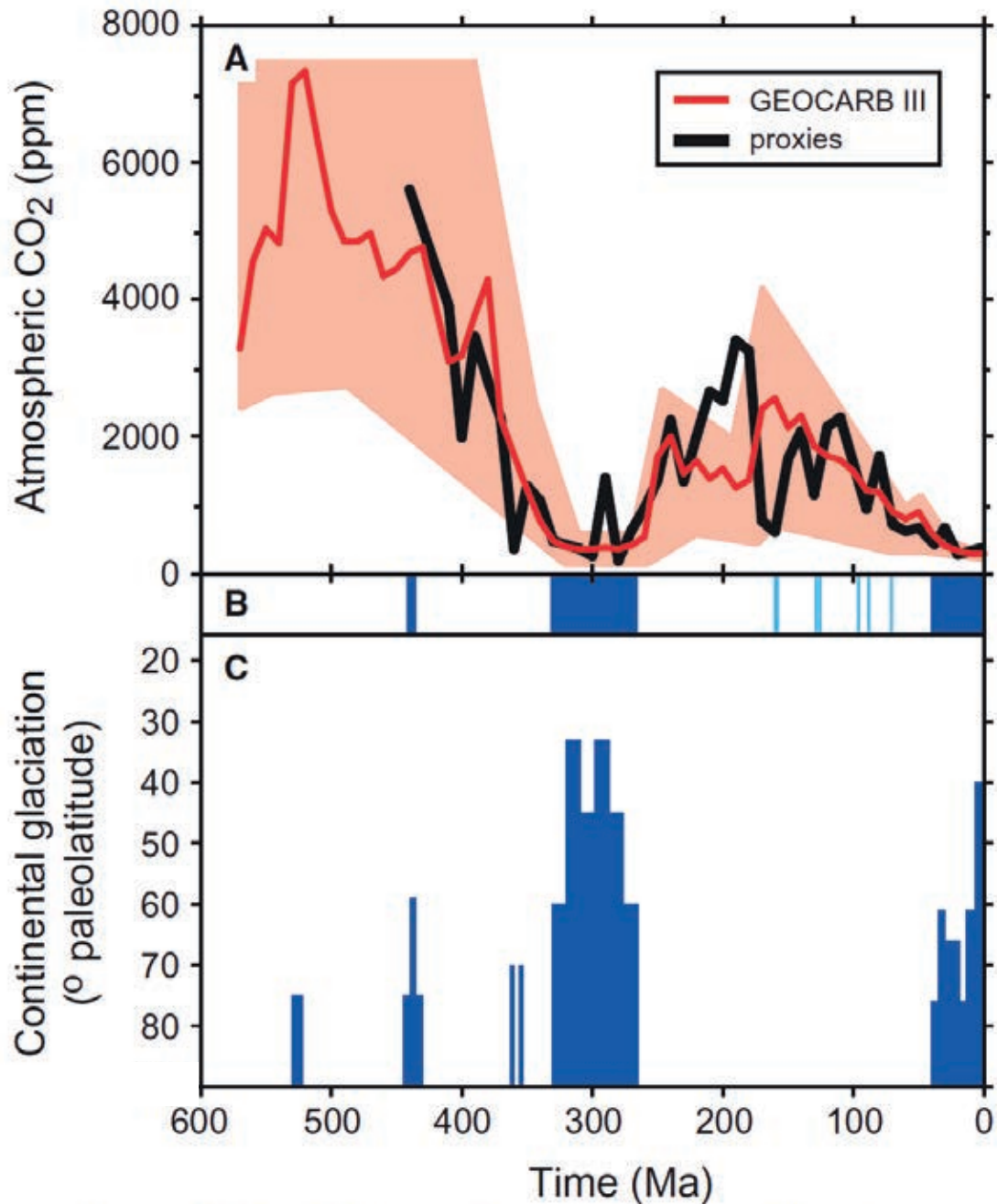


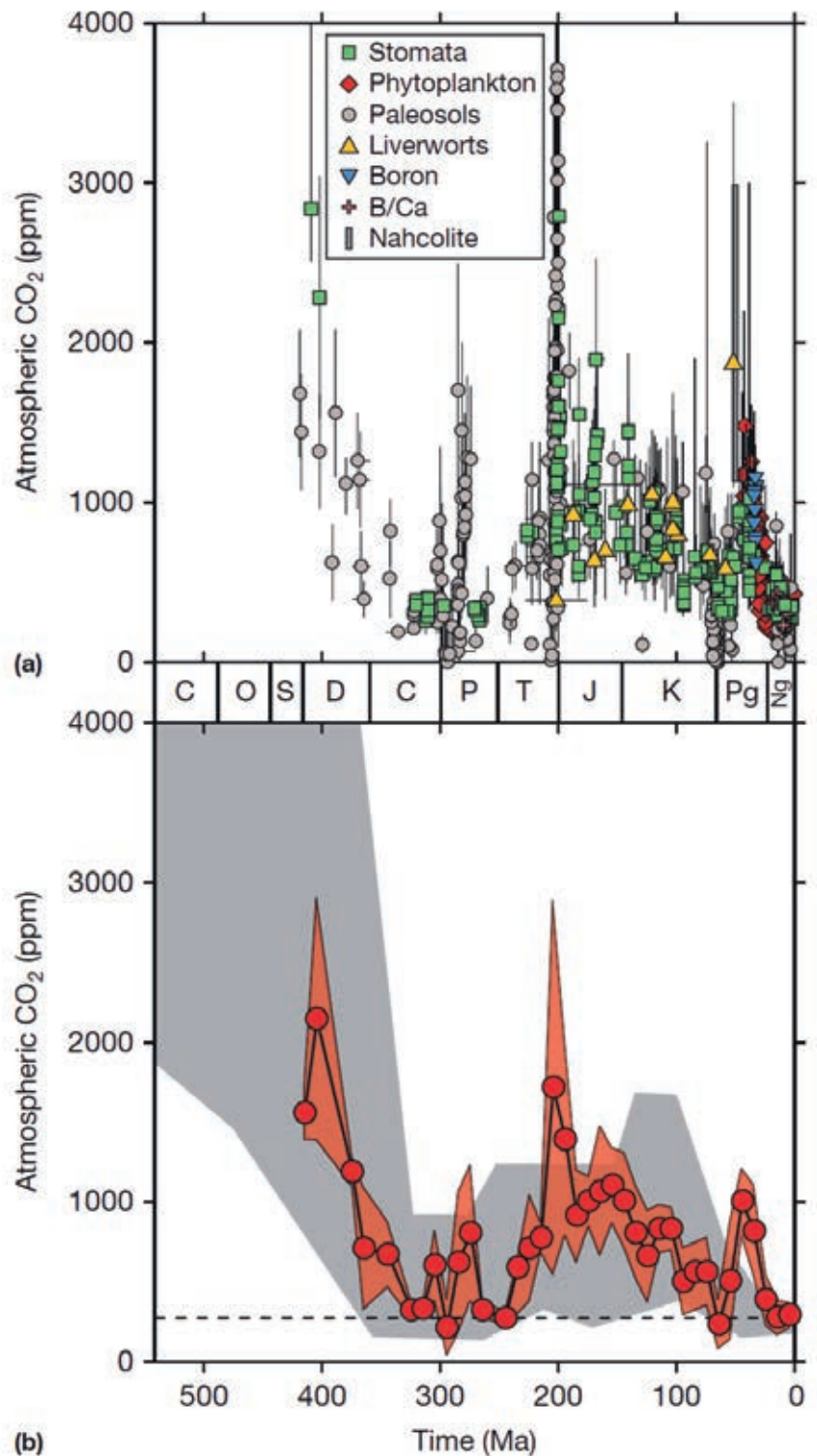
Figure 2. CO₂ and climate. **A:** Comparison of model predictions (GEOCARB III; Bernier and Kothavala, 2001) and proxy reconstructions of CO₂. 10 m.y. time-steps are used in both curves. Shaded area represents range of error for model predictions. **B:** Intervals of glacial (dark blue) or cool climates (light blue; see text). **C:** Latitudinal distribution of direct glacial evidence (tillites, striated bedrock, etc.) throughout the Phanerozoic (Crowley, 1998).

DOCUMENT 11 : Estimations de la pCO₂ atmosphérique à l'échelle du Phanérozoïque

GEOCARB : Courbe synthétique (modélisation) de l'évolution de la pCO₂ (Berner et Kothavala, 2001)

Liverwort : hépatique
Nahcolite : NaHCO₃

Source : Royer DL, Berner RA, Montan ez IP, Tabor NJ, and Beerling DJ (2004) CO₂ as a primary driver of Phanerozoic climate. *GSA Today* 14(3): 4–10.



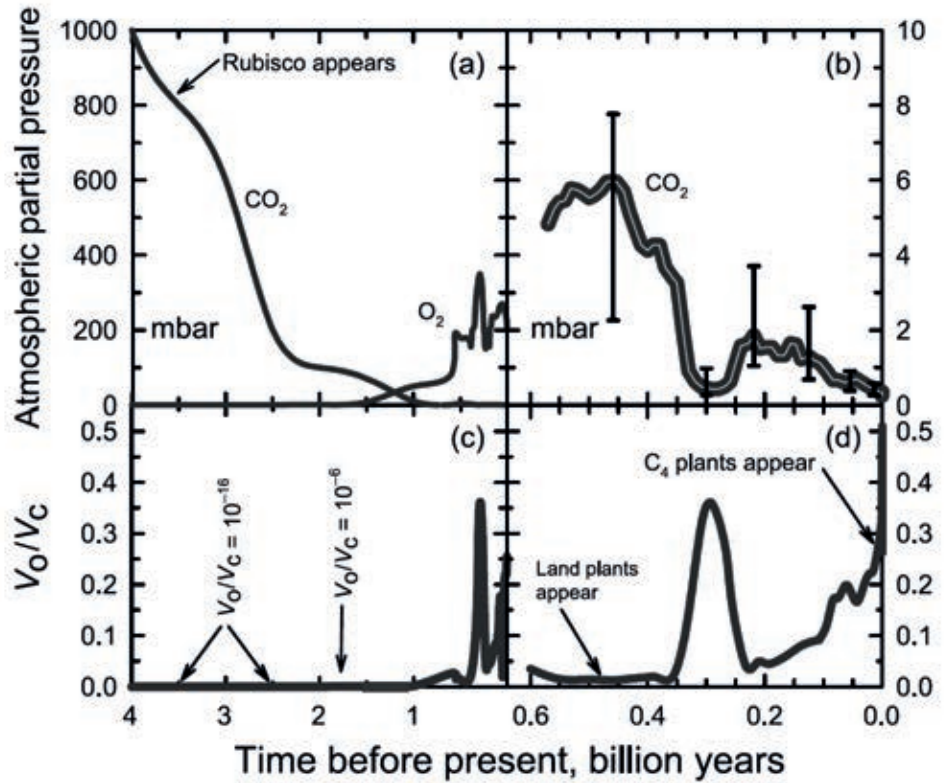
Phanerozoic history of atmospheric CO₂ from proxies. (a) Individual CO₂ estimates, coded by proxy type ($n=761$). See [Table 1](#) for data sources. Some estimates from [Schaller et al. \(2011\)](#) near the T/J boundary exceed 4000 ppm and are not visible. (b) CO₂ estimates averaged into 10 My bins (red circles). Bins represented by single estimates are excluded; red band captures $\pm 1\sigma$ of the binned data set. The 10 My time step allows a cleaner comparison to the GEOCARB output (gray band, from [Figure 2\(a\)](#)), which has the same time step.

La teneur en CO₂ de l'atmosphère : marqueur des flux entre la biosphère et les autres réservoirs du cycle de carbone.

DOCUMENT 12 : pCO₂ et potentiel d'oxygénation de la Rubisco des plantes en C₃ à l'échelle des temps géologiques

Source : Sage, R, F, 2003, *The evolution of C₄ photosynthesis*, *New Phytologist* (2004) 161: 341–370

Profiles of modeled atmospheric CO₂ and O₂ partial pressures (in mbar) over the history of the earth (a,b), and corresponding estimates of relative oxygenation potential for C₃ photosynthesis (c,d). Atmospheric CO₂ levels were modeled over the past 4 billion years (a) and 0.6 billion years (b); atmospheric O₂ levels were modeled over the past 4 billion years (data from Berner 1994). Oxygenation potential is modeled as the ratio of RuBP oxygenation to carboxylation (V_O/V_C) corresponding to the gas levels shown in (a,b) and assuming a C₃ Rubisco (from spinach) at 30°C. from Sage (1999) by permission.

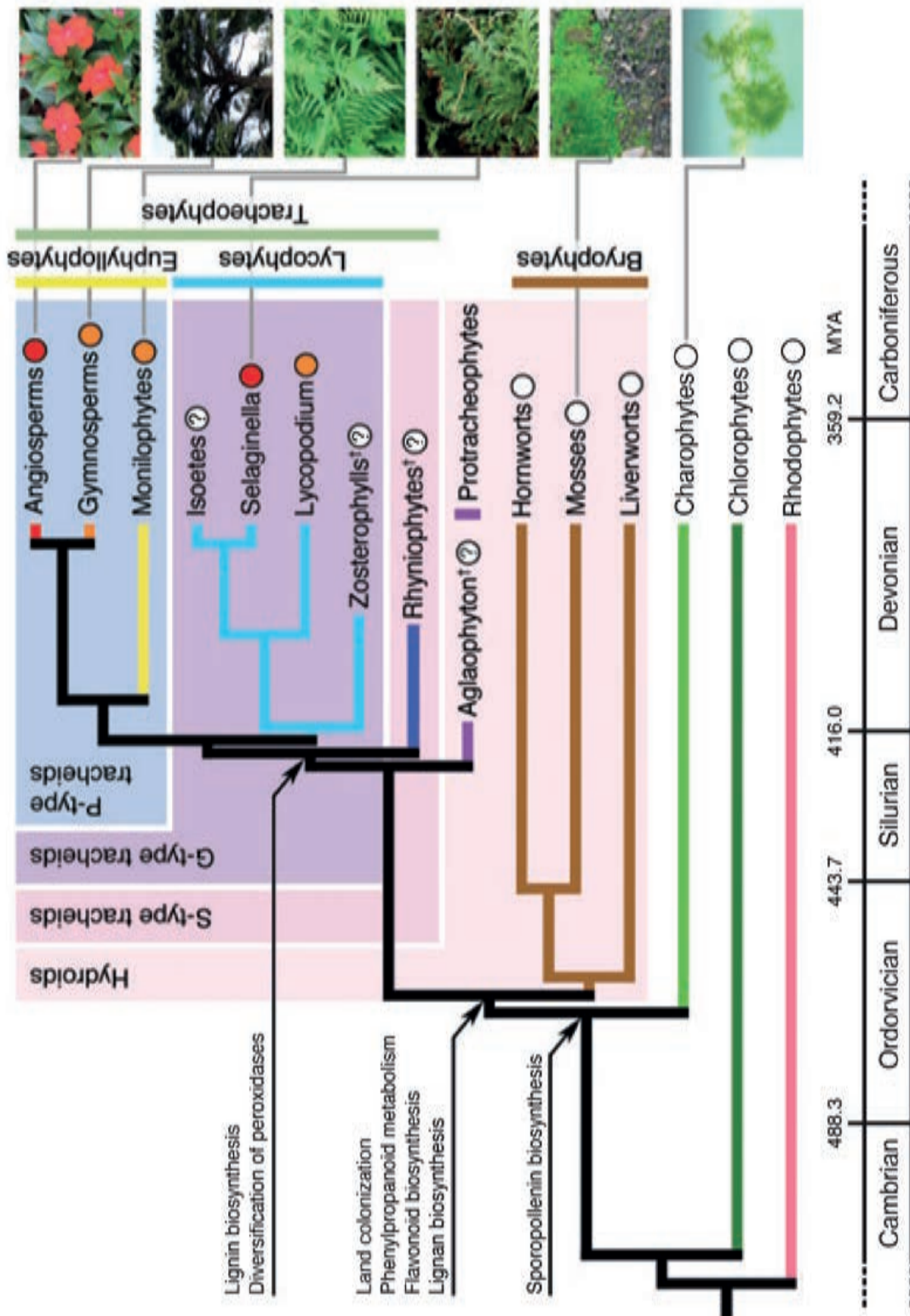


La teneur en CO₂ de l'atmosphère : marqueur des flux entre la biosphère et les autres réservoirs du cycle de carbone.

DOCUMENT 13 : La phylogénie des plantes et la biosynthèse de la lignine.

Les lignanes (lignans) sont des composés polyphénoliques différents des lignines.

Source : Wend J. K. and C. Chapple, 2010, *The origin and evolution of lignin biosynthesis*, *New Phytologist* (2010) 187: 273–285



A plant phylogenetic tree marked with the major milestones of evolution of lignin biosynthesis. The distribution of lignin and its monomeric composition across major plant lineages are denoted by a circle at each branch. Open circle, no lignin; orange circle, presence of H and G lignin; red circle, presence of S lignin in addition to H and G lignin; circle with question mark, unknown. Note that, within several groups with G lignin, S lignin-containing exceptions are known. †Extinct lineage.